PREDICTION OF EARTH PRESSURES ON CONCRETE RETAINING WALLS FROM SURFACE LINE LOADS

A.T.C. GOH[1]

SYNOPSIS

The lateral pressures acting on the wall stem from externally applied line loads for concrete cantilever retaining walls is considered. These lateral pressures are of concern as the design of the structural components of these retaining walls is greatly influenced by the lateral earth pressures acting on the wall stem. Detailed studies were carried out using the finite element method in which the stage-by-stage construction of the wall and backfill placement were simulated. The soil was modeled by an elastic-ideally plastic constitutive relationship, while the interface elements at the concrete-soil interface were modeled by a hyperbolic constitutive relationship. The lateral pressures predicted by the finite element method differed from the predictions from conventional techniques based on elastic theory. These differences can be attributed to the erroneous implication in elastic theory that any combination of effective principal stress ratio is possible for the backfill soil.

INTRODUCTION

Most existing methods for designing gravity type retaining structures are essentially based on the theoretical formulations of Coulomb (1776) and Rankine (1857). These methods generally rely on the assumption that sufficient, arbitrary lateral yield will occur to fully mobilize active conditions behind the wall. Furthermore, the construction sequence is usually not considered, with most walls in illustrative problems appearing magically in place without apparent construction disturbance of the natural soils. No account is also taken of the deformation properties of the backfill and foundation subsoils, the flexibility of the wall or the soil-structure interaction between materials with disparate stress-strain characteristics.

With the use of the finite element method, more realistic consideration of many of the factors as well as material nonlinearity have become feasible. The finite element method also has the added advantage of being able to provide predictions of stresses and displacements under working load conditions, whereas limit equilibrium solutions generally only provide information related to the ultimate failure condition. Clough and Duncan (1971) were one of the first to study the behavior of gravity retaining walls using the finite element method. Their analysis of a 6.1 m high gravity retaining wall in which the stage-by-stage construction sequence of the sand backfill and the

[1] Senior Lecturer, School of Civil Engineering & Building, Swinburne University of Technology, Melbourne, Australia 3122.

soil-structure interaction were simulated, indicated that the horizontal earth pressures acting on the wall were in excess of the active pressures. Similar findings were obtained by Kulhawy (1974) in his analysis of a 31.8 m high gravity retaining wall for a hydroelectric project. In both studies, the higher than active earth pressures were attributed to insufficient wall movements away from the backfill. The influence of the type and magnitude of the wall movements on the lateral earth pressures were also verified by more recent numerical studies by Nakai (1985), and Bakeer and Bhatia (1989). The importance of the soil-structure interaction effects on the behavior of gravity retaining walls were highlighted recently through finite element studies by Duncan et al. (1990).

Todate, very limited numerical studies have been carried out to investigate the behavior of concrete cantilever walls. The results presented in this paper are part of an ongoing project to examine the behavior of concrete cantilever retaining walls using the finite element method. In a forthcoming paper, Goh (1993) examined the behavior of concrete cantilever walls (with no externally applied loads) through detailed parametric studies of a wide range of cantilever retaining walls. This work has been extended to focus on the effects of vertical surcharge line loads acting on the surface of the backfill and the prediction of the lateral stresses acting on the wall stem under working load conditions, and is the subject of this paper.

REVIEW OF CONVENTIONAL METHODS

For a surcharge line load placed at the surface of the backfill of a gravity type retaining wall, most textbooks and design Codes rely on the theory of elasticity to compute the lateral pressures acting on the wall back. Fig 1 (a) illustrates a typical design method found in many textbooks. The equations for the lateral pressure (p) were derived from elastic theory with the assumption that the wall is unyielding and rigid, and then slightly modified to agree with experimental findings (Terzaghi, 1954). As pointed out by Clayton and Mililitsky (1986), the main criticism of this approach for determining the horizontal pressure acting on the wall relates to the implicit assumption that the strength of the soil is infinite. This implies that any combination of effective principal stress ratio is possible for the backfill soil. In reality, the effective principal stress ratios are limited to less than, or equal to, the value at which failure occurs. This constraint has particular relevance for gravity and semi-gravity retaining walls since the backfill in the vicinity of the wall back is usually in the active (failure) condition as highlighted by the finite element analyses presented later.

Another common approach is the empirical technique suggested by CP2 (1951) based on Terzaghi and Peck (1948) and shown in Fig. 1 (b). The line load Q is considered to exert a horizontal force of magnitude Ka.Q on the wall with its point of application as indicated. This method which is essentially based on the Coulomb wedge graphical approach gives results entirely different from experimental findings (Terzaghi, 1954).
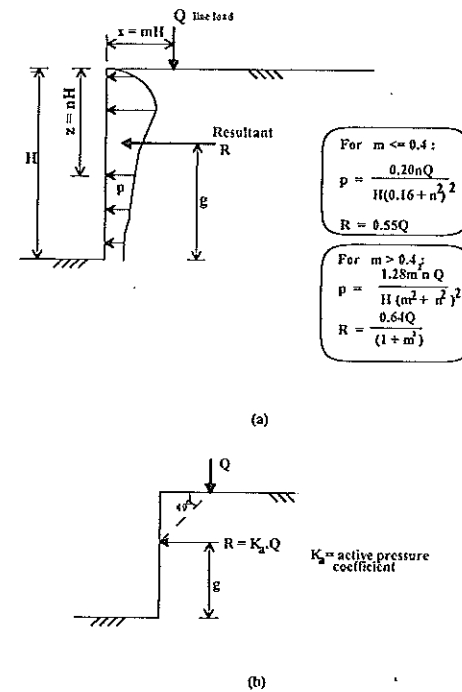
Fig. 1 (a) Horizontal Pressures from Line Load using Elastic Method (b) Approximate Method

NUMERICAL TECHNIQUE

Fig. 2 shows the wall configuration used in this study. Table 1 summarizes the details of the wall dimensions and properties, and the soil properties. The strength and initial stiffness properties of the foundation subsoil and backfill soil are essentially similar to those used by Clough and Duncan (1971).

The basic finite element mesh and the displacement boundary conditions are depicted in Fig. 3, with the elements concentrated in the zones of high stress gradients. The vertical right boundary was sufficiently remote to represent an infinitely long backfill. A plane-strain finite element program was used in the analyses. The program essentially followed the 'initial stress' finite element formulations of Nayak and Zienkiewicz (1972). Eight-noded isoparametric elements with reduced integration were used to model the soil and wall elements. The soil was modeled as linear elastic-perfectly plastic with a Mohr-Coulomb yield surface, and associated flow conditions have been assumed. The wall was assumed to behave linear elastically.
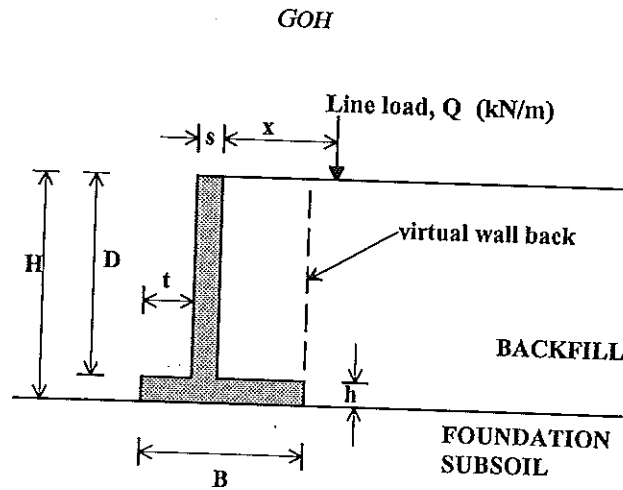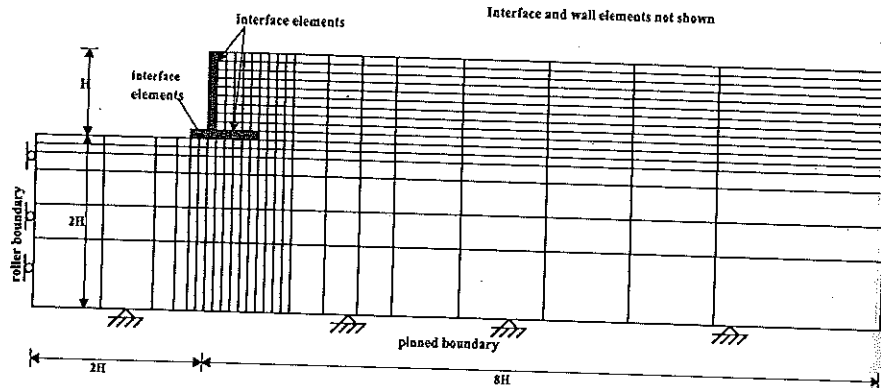
Fig. 2 Retaining Wall Geometry

Fig. 3 Finite Element Mesh

Six-noded interface elements based on the Goodman et al. (1968) model were employed to model the interaction between the soil and the structure. The interface shear stress-displacement constitutive model adopted was essentially similar to the model used by Clough and Duncan (1971). The interface normal stiffness was assigned a high arbitrary value of 1×10^6 MPa/m to prevent overlap of the adjacent two-dimensional solid elements. The tangent stiffness K_{st}, which is the slope of the interface shear stress-displacement curve is expressed as

$$K_{st} = K_s . (1 - R_f . SL)^2 \tag{1}$$

where K_s is the initial shear stiffness, R_f is the failure ratio and SL is the interface stress level and represents the proportion of the mobilized interface shear strength. In this study, K_s was assigned a value of 490 MPa/m for the interface elements directly beneath the wall base. This value is of the same order of magnitude as experimental values obtained from concrete-sand interface direct shear tests by Clough and Duncan (1971) and Acar et al. (1982). The effects of a lower K_s value are considered later. When the shear strength of the interface is exceeded, the shear stiffness was assigned a small value of 0.01 MPa/m, while maintaining the high normal stiffness. The interface elements in contact with the backfill ie. at the back of the wall stem and above the wall heel were assigned small K_s values of 0.001 MPa/m in order to simulate a perfectly smooth contact between the wall and the backfill. Only the analyses assuming a perfectly smooth wall back are presented here as the analyses with a rough wall back indicated the same trends and have been omitted.

The stage-by-stage placement of the wall and backfill were simulated using the technique proposed by Clough (1969). The cohesionless backfill was assumed to be loosely placed or very lightly compacted with $K_o = 1 - \sin \phi$. Compaction effects such as the finite element simulation procedures proposed by Seed and Duncan (1986) were not considered. The analysis was carried out in 12 increments for the placement of the wall and backfill and 3 increments for the applied line load. The norm of displacement changes criterion (Nayak and Zienkiewicz 1972) was used to ensure sufficient accuracy of the solution before the iterative process is terminated. Convergence was assumed when the change in nodal displacements, non-dimensionalized with respect to the largest absolute value, nowhere exceeded 0.1%.

FINITE ELEMENT ANALYSES

Finite element analyses were carried out on both a 3 m high and a 6 m high concrete cantilever retaining wall. Different magnitudes of Q as well as distance (x) of Q away from the wall back were considered, and the details are summarized in Table 2. It should be noted that in any computations of the retaining wall safety factors against sliding and overturning, it is the horizontal stresses acting on the vertical plane passing through the heel of the wall (virtual back) that are of major concern. However as emphasized earlier, the main focus in this paper is on the stresses acting on the wall stem under practical working load conditions. In the problems analysed, the factors of safety based on CP2 (1951) were between 1.45 and 1.75 for sliding failure, and between 2.0 and 3.0 for overturning failure. The lateral stresses acting on the wall stem are generally of interest for the structural design of the reinforced concrete wall. One common practice in design is to modify the lateral pressures acting on the wall stem by multiplying the pressure by a load factor which usually has a value greater than unity.

Wall Displacement

Typical displacements of the wall are presented in Fig. 4. Fig. 4(a) shows the predicted wall displacements at the completion of backfilling and at the end of the application of the external load (Case CWL2 : Q = 15 kN/m, x = 0.8 m) on an exaggerated scale. Fig. 4(b) shows the corresponding vector nodal displacements of the top and bottom of the wall stem on an exaggerated scale. The vectors at three different stages are shown : (1) backfilling to a height of 1.8 m above the wall base, (2) at the completion of backfilling (3 m of fill placement), and (3) after the application of the external line load.
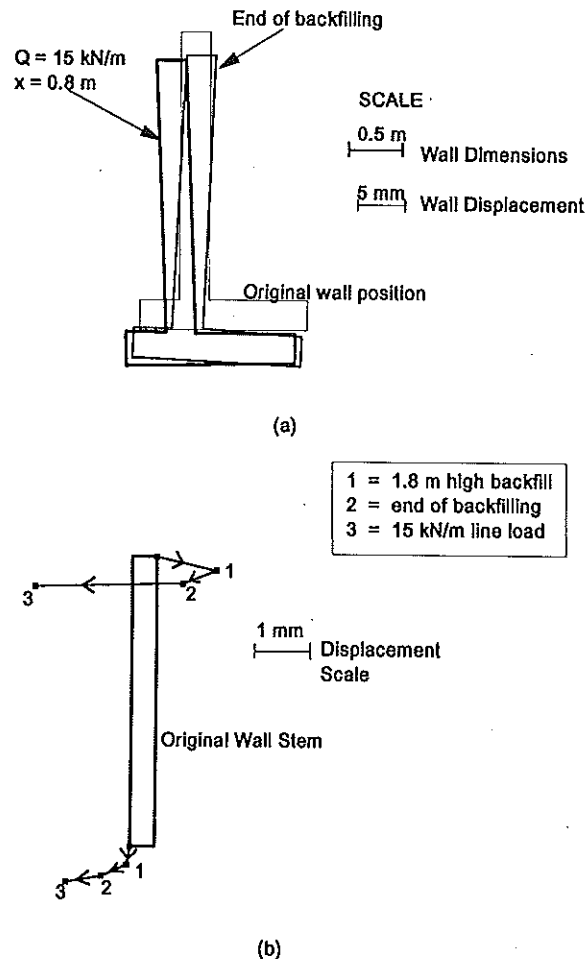

(a)

(b)

Fig. 4 (a) Wall Movements (b) Nodal Displacements of Wall Stem

In the initial stages of the fill placement, the weight of the fill placed on top of the wall heel caused settlement of the heel and resulted in the top of the wall moving into the backfill. With further gradual fill placement, the lateral pressures exerted on the wall stem from the additional layers of fill resulted in the gradual lateral yielding of the stem. This caused the top of the wall stem to translate and tilt away from the backfill. The base of the wall also translated away from the backfill as shown in Fig. 4(a). At the completion of the backfill placement, the settlement of the wall base was greater at the heel than at the toe, due to the larger settlement of the foundation subsoil in the vicinity of the heel than at the toe. These results are consistent with the gravity retaining wall analyses of Clough and Duncan (1971) and Kulhawy (1974), and the centrifuge tests on bridge abutments (Bolton et al. 1990).

As expected, the subsequent application of the line load resulted in further rotation and translation of the wall stem and base away from the backfill. This caused the settlement of the wall toe to be larger than the settlement of the wall heel. Analyses carried out for line loads at greater distances away from the wall back (CWL3 and CWL4) indicated the same trends in the wall displacements and are not shown. However, as expected, the magnitudes of the movements were smaller the further the line load was away from the wall back.

Earth Pressures

The predicted lateral pressures acting on the wall back for two values of Q and three values of x (CWL2 to CWL7) are shown in Fig. 5. z is the depth of the soil below the top of the backfill. The theoretical at-rest and Rankine active earth pressures (Q = 0) as well as the finite element lateral pressures at the end of backfilling (CWL1) are also shown. At the end of backfilling, the predicted lateral pressures correspond closely to the classical Rankine active pressures for the top two-thirds of the wall. In the lower third of the stem, the predicted lateral pressures are significantly in excess of the active pressures, because of insufficient lateral yielding of the wall stem (Goh, 1993).

The applied load resulted in significantly larger lateral pressures on the wall stem when the line load is close to the wall back (CWL2, CWL3 and CWL5). The results suggest that the lateral pressures are influenced by the magnitude and line of action of the line load. For CWL2 and CWL5, the lateral pressures close to the bottom of the wall stem are smaller than at the end of backfilling (CWL1). This is likely to be due to the horizontal stress release from the lateral movement of the wall away from the backfill after the line load is applied.

The line load resulted in significant increases in both the horizontal and vertical stresses. This is demonstrated for one of the load cases (CWL2) in Fig. 6 which shows the typical distributions of the horizontal and vertical pressures with distance (d) away from the wall stem. Two different depths (z) below the top of the backfill, representative of the soil close to the top of the backfill (z/H = 0.15) and in the middle of the backfill (z/H = 0.45) are shown. Also included for comparison are the stresses at the end of backfilling (CWL1) prior to the line load application. As shown in Fig.
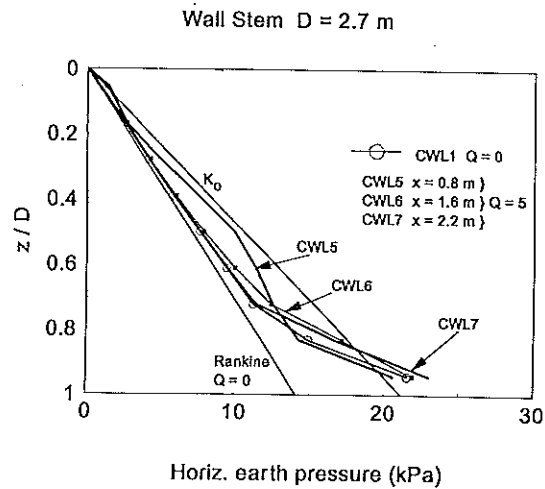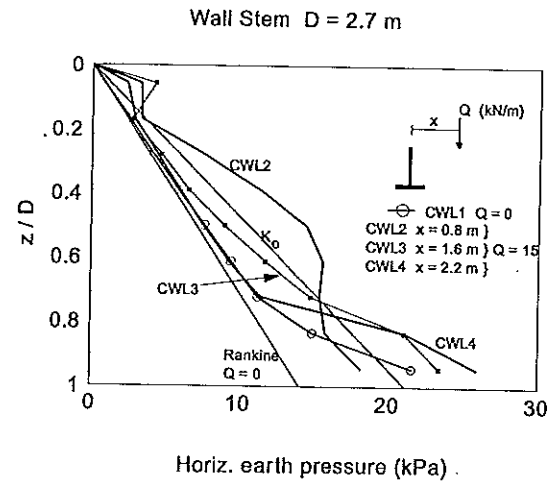
Wall Stem D = 2.7 m

Horiz. earth pressure (kPa)

Wall Stem D = 2.7 m

Horiz. earth pressure (kPa)

Fig. 5 Lateral Earth Pressure Distributions at the Wall Stem (D = 2.7 m)

6, at the completion of backfilling, the horizontal stresses gradually increase with distance away from the wall stem while the vertical stresses decrease gradually with increasing d/H. With the application of the line load, there is a concentration of horizontal and vertical stresses close to the point of application of the load.
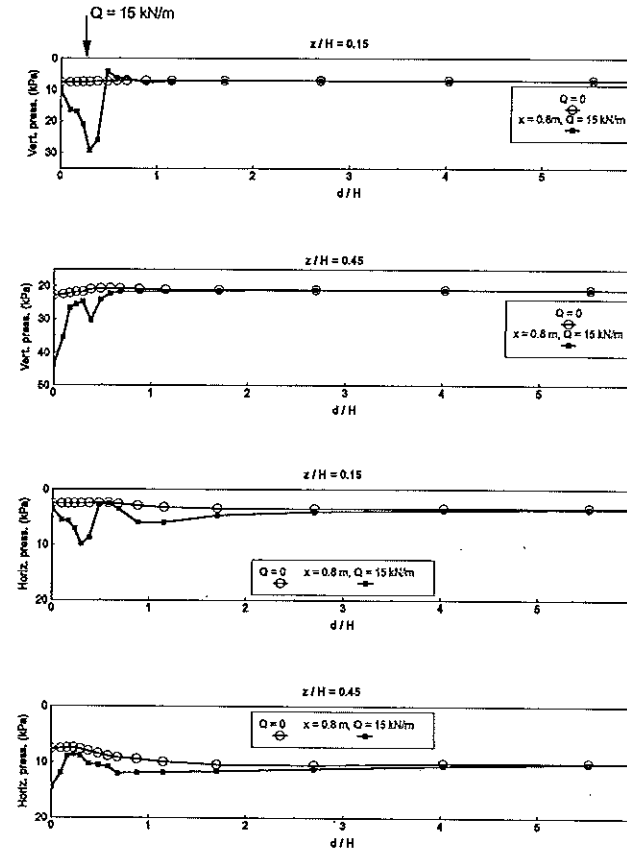
Fig. 6 Horizontal and Vertical Pressure Profiles (CWL2)

Stress Paths

Typical stress paths of the backfill soil are presented in Fig. 7 for CWL2. The stress paths of four elements are shown. Element A is the soil element adjacent to the wall heel. Element B is the soil element adjacent to the base of the wall stem. Elements C and D are at mid-height in the backfill. The open symbols show the stress paths to the end of the backfilling while the shaded symbols show the stress paths when the line load is applied. During the backfilling, the stress paths for these four elements indicate an increase in shear stress (q') and mean effective stress (p') with increasing backfill placement. For element C, the stress condition of the element after reaching failure moves upward along the failure line. For element D, the stress path is almost parallel to the failure line. For elements A and B, the stress paths show that while the placement of additional layers of fill increased the vertical pressures, the reductions in the horizontal pressures were minimal.
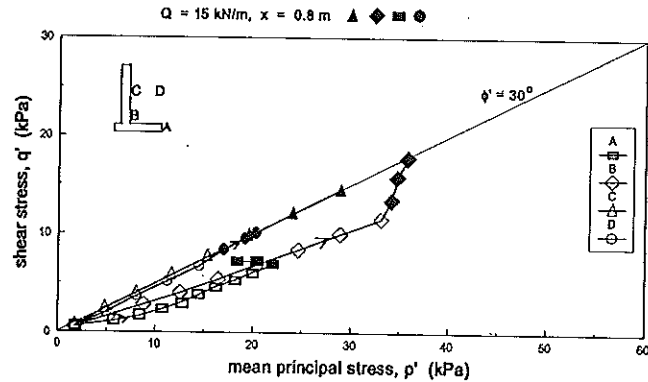
Q = 15 kN/m, x = 0.8 m ▲ ◆ ▣ ◉

Fig. 7 Stress Path Plots (CWL2)

With the application of the line load, for element C, the stress path continued to move upward along the failure line. For elements B and D, the increased shearing resulted in the stress paths moving upward and to the right, indicating increases in both vertical and horizontal incremental stresses, until they reached the failure line. For element A, the stress path moved almost horizontally towards the left indicating a proportionate decrease in both the vertical and horizontal incremental stresses. This stress release is likely to be due to the horizontal translation of the wall base away from the backfill.

Parametric Studies

Further finite element studies were carried out to investigate the influence of the wall and interface properties on the lateral pressures acting on the wall stem. The properties of the backfill soil and foundation subsoil previously assumed in Table 1 were used.

Fig. 8 shows the lateral earth pressures for a 6 m high wall with $D = 5.4$ m, $B = 3.4$ m, $s = 0.6$ m, $h = 0.6$ m and $t = 0.8$ m. Four cased were considered : (1)
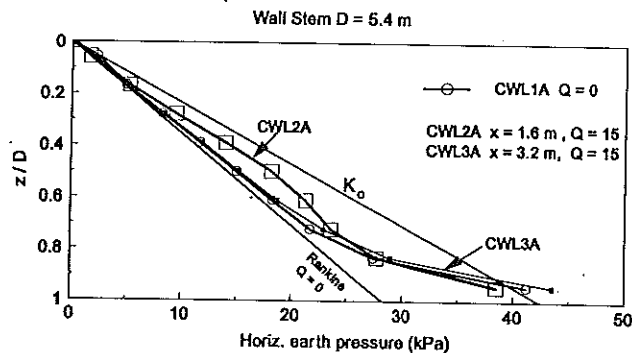

Fig. 8 Lateral Earth Pressure Distributions at the Wall Stem (D = 5.4 m)

Table 1 Properties Employed in Finite Element Analyses

Property	Symbol	Value
Wall Properties		
Wall base width (m)	B	1.7
Wall toe width (m)	t	0.4
Wall stem thickness (m)	s	0.3
Wall heel thickness (m)	h	0.3
Wall height (m)	H	3.0
Wall stem height (m)	D	2.7
Young's modulus (x 10^3 MPa)	E_c	25
Poisson's ratio	υ_c	0.2
Unit weight (kN/m^3)	γ_c	22.0
Backfill Soil		
Elastic modulus (MPa)	E_b	40
Poisson's ratio	υ_b	0.33
Friction angle	ϕ_b	30°
Cohesion (kPa)	c	0
Unit weight (kN/m^3)	γ_b	15.7
Coefficient of earth pressure at-rest	K_o	0.5
Foundation Subsoil		
Elastic modulus (MPa)	E_f	70
Poisson's ratio	υ_f	0.30
Friction angle	ϕ_f	35°
Cohesion (kPa)	c	0
Unit weight (kN/m^3)	γ_f	18.0
Coefficient of earth pressure at-rest	K_o	0.426
Wall Base Interface		
Initial shear stiffness (MPa/m)	K_s	490
Failure ratio	R_f	0.9
Friction angle	δ_f	30°

CWL1A (Q = 0), (2) CWL2A (Q = 15 kN/m, x = 1.6 m), (3) CWL3A (Q = 15 kN/m, x = 3.2 m) and (4) CWL4A (Q = 15 kN/m, x = 4.4 m). For CWL2A, CWL3A and CWL4A, the same normalized distance (m) of 0.296, 0.593 and 0.815 were used as for CWL2, CWL3 and CWL4 respectively. The lateral pressures predicted for CWL4A were marginally smaller than for CWL3A and therefore have been omitted. A comparison of Fig. 5 and Fig. 8 indicate that for the same m value, the increase in lateral pressures for the 6 m high wall are smaller than for the 3 m high wall.

The effects of the stiffness properties of the wall and the wall base interface shear stiffness K_s on the lateral pressures are shown in Fig. 9. Also shown are the results from CWL2. For CWL2B, the Young's modulus (E_c) of the wall was increased a thousand times to 25000 GPa to simulate a very rigid wall. For CWL2C, E_c was reduced to a tenth of the value for CWL2 to 2500 MPa to simulate the situation of a cracked concrete wall. These two cases represent two extreme situations. In practice, the cracking of the concrete is likely to reduce the bending stiffness by about half. The value of K_s of 49 MPa/m used for CWL2D which is a tenth of the value used in CWL2, would probably be indicative of the lower bound value for concrete-sand interface shear stiffness. For all these cases, Q = 15 kN/m and x = 0.8 m were assumed. The differences in the lateral pressures acting on the wall stem as illustrated in Fig. 9 are marginal.

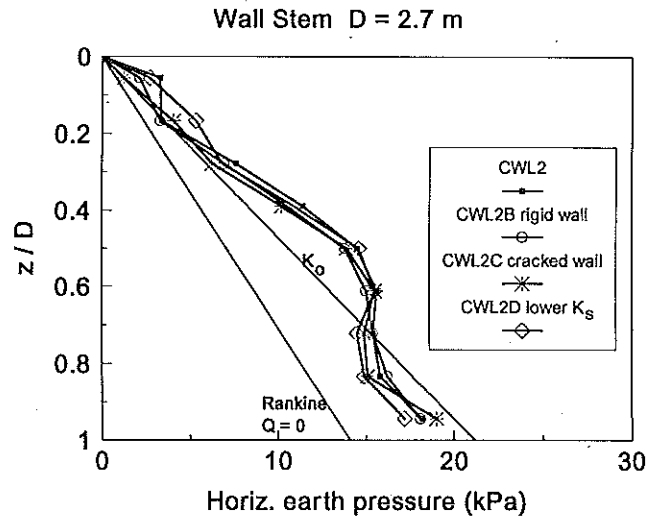**Fig. 9 Lateral Earth Pressure - Varying Wall and Interface Stiffness Properties**

COMPARISON WITH CONVENTIONAL METHODS

Lateral Earth Pressure Profile

The above finite element results indicate that the lateral pressures acting on the wall stem are influenced by the magnitude of the line load and the point of application of the load. Also of interest is the increase in pressure (p) due to the application of the line load. This was obtained by subtracting the lateral pressures after the line

load is applied from the lateral pressures at the completion of backfilling. Fig. 10 shows the non-dimensionalized plots of the results from Fig. 5 together with the results obtained using the theory of elasticity as outlined earlier in Fig. 1(a). In some cases, negative values of p were computed close to the base of the wall stem. As mentioned previously, this was because the lateral pressures after the application of the line load were smaller than the pressures at the end of backfilling. A comparison of the results indicates wide variations in the pressure profiles predicted using the finite element method and from elastic theory.

Similar differences between the predictions from the finite element method and elastic theory were obtained for the results shown in Fig. 8 and Fig 9. These results
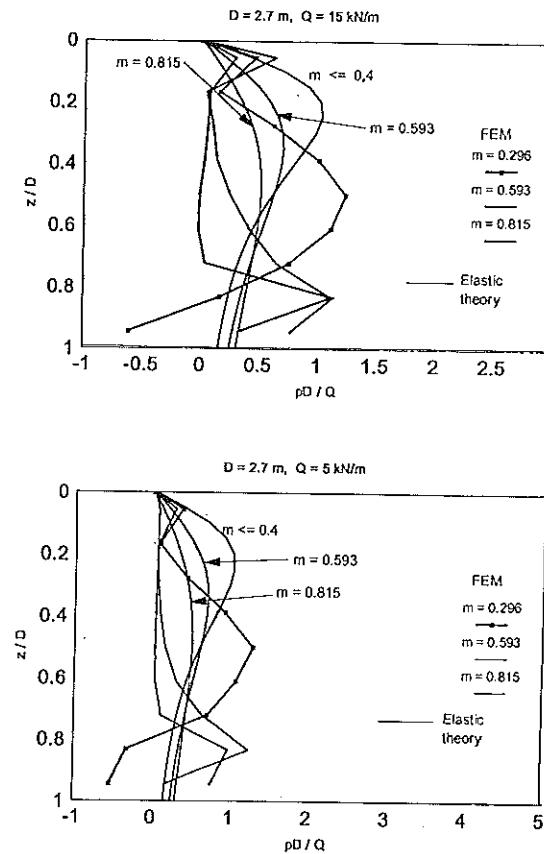

Fig. 10 Normalized Lateral Earth Pressures (D = 2.7 m)

are non-dimensionalized in Fig. 11 and Fig. 12. It can be seen from Fig. 12 that for the same values of m, the pressure profiles have the same general shape irrespective of the wall properties and magnitude of Q.

In elastic theory the backfill soil is assumed to possess infinite strength. As mentioned earlier, this implies that any combination of effective principal stress ratio is possible for the backfill soil. In reality, the effective principal stress ratios are limited to less than, or equal to, the value at which failure occurs. This accounts for
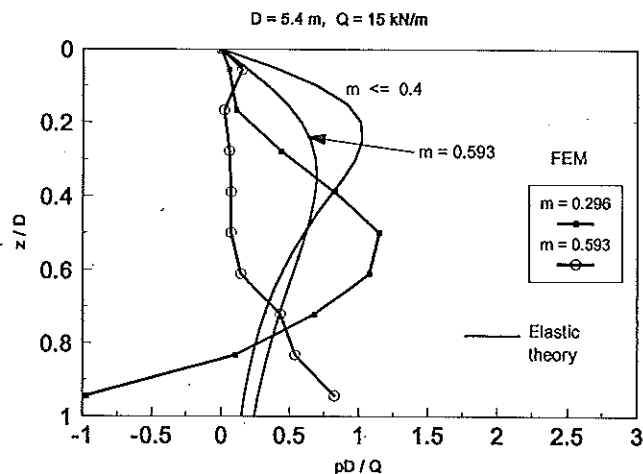

Fig. 11 Normalized Lateral Earth Pressures (D = 5.4 m)

the differences in the predictions between the finite element and elastic methods. For the retaining walls analysed, and for most gravity type retaining walls in general, at the completion of backfilling, most of the backfill soil in the vicinity of the wall back is in the active (failure) condition. For example, Fig. 13 shows the plot at the completion of backfilling (CWL1) of the elements where the proportion of mobilized shear strength (stress level) is greater than 0.99, essentially defining the failure zone. With the application of the line load, the increase in the horizontal and vertical pressures for the elements in this 'failed' region were limited and resulted in a redistribution of the excess stresses to the elements immediately outside this region that were not at failure such as the soil directly above the wall heel. Consequently, this caused some of the elements directly above the wall heel to fail as shown in Fig. 13 for CWL2.

Equivalent Horizontal Load

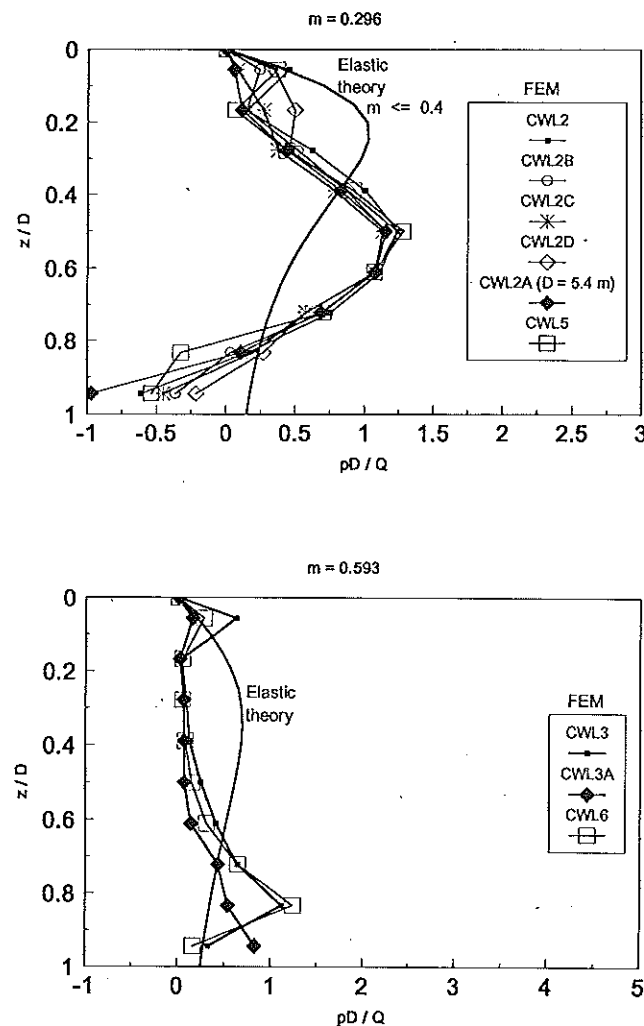One simplistic procedure for considering the effects of a line load is to assume

Fig. 12 Normalized Lateral Earth Pressures (a) m = 0.296 (b) m = 0.593

an equivalent horizontal load acting on the wall back. One such technique has been described earlier in Fig. 1(b). In this section, the finite element predictions are compared with the results from this approximate method and from elastic theory. The normalized horizontal resultant force (R) and the line of action (g) of the resultant with respect to the base of the wall stem are summarized in Table 2 and plotted in Fig. 14.
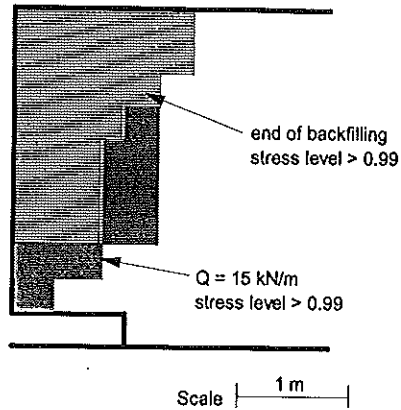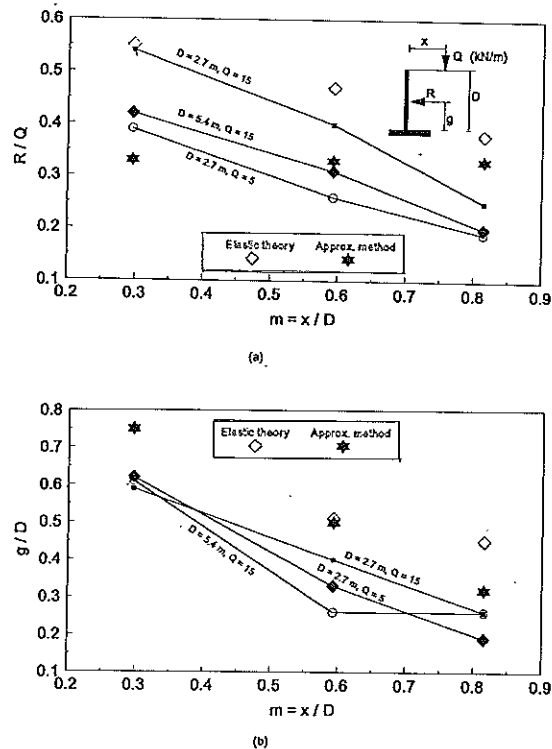
Fig. 13 Plot of Stress Levels (CWL2)

(a)

(b)

Fig. 14 Comparison of Results of Resultant Force

Table 2 Comparison of Results of Resultant Force

Case	D (m)	Q (kN/m)	m = x/D	Resultant Horiz. Load (R / Q)	Line of Action of Resultant from Base of Stem (g / D)
Elastic theory	2.7	15	0.296	0.55	0.60
Approx. method				0.33	0.75
CWL2				0.54	0.59
Elastic theory	5.4	15	0.296	0.55	0.60
Approx. method				0.33	0.75
CWL2A				0.39	0.61
Elastic theory	2.7	5	0.296	0.55	0.60
Approx. method				0.33	0.75
CWL5				0.42	0.62
Elastic theory	2.7	15	0.593	0.47	0.51
Approx. method				0.33	0.50
CWL3				0.40	0.40
Elastic method	5.4	15	0.593	0.47	0.51
Approx. method				0.33	0.50
CWL3A				0.26	0.26
Elastic method	2.7	5	0.593	0.47	0.51
Approx. method				0.33	0.50
CWL6				0.31	0.33
Elastic method	2.7	15	0.815	0.38	0.45
Approx. method				0.33	0.32
CWL4				0.25	0.25
Elastic method	5.4	15	0.815	0.38	0.45
Approx. method				0.33	0.32
CWL4A				0.19	0.26
Elastic method	2.7	5	0.815	0.38	0.45
Approx. method				0.33	0.32
CWL7				0.20	0.19

From these results, the following conclusions can be made:

(1) For the finite element method, both R and g increased with increasing Q and decreasing m. Reducing Q to a third resulted in a 20% reduction of R. R and g

are also affected by the height of the wall stem D. Doubling the wall height resulted in a reduction of R of approximately one third.

(2) In the elastic method, R and g also increased with increasing Q and decreasing m. However, R is independent of D. This appears unrealistic. For example, a wall with D = 2.7 m and x = 1 m would give the same magnitude for R as a wall with D = 5.4 m and x = 2 m since m is the same in both cases. It seems reasonable to expect that the latter should give a smaller R since the line load is further away from the wall stem. This is in fact confirmed from finite element analyses. The results however have been omitted from this paper as they did not reveal any further insights. The elastic method predictions for R were larger than the finite element predictions for all nine cases considered. These differences varied between about 3% and 60%. For the three cases where m = 0.296, the values of g obtained by both methods were in close agreement. In all the other cases, the elastic method predictions for g were at least 20% higher than the finite element predictions. This suggests that the elastic method can lead to very conservative estimates of the resultant.

(3) The approximate method appears unrealistic as it leads to values of R that are independent of m and D. The predictions for g were at least 20% higher than the finite element predictions. No distinct trend could be observed with regards to R although for m = 0.296, the approximate method resulted in smaller values than the finite element predictions.

CONCLUSIONS

The finite element method has been used to examine the behavior of concrete cantilever retaining walls subjected to external line loads. The investigations indicate substantial variations in the lateral pressures obtained using the finite element method and conventional design techniques. The finite element allows for more realistic considerations of the soil-structure interaction, material nonlinearity and the construction sequence, and should lead to solutions that are closer to real situations than conventional design methods. Although experimental verification of the numerical findings is not available, these analyses should provide sufficient qualitative insights and guidelines for the development of improved design methods.

REFERENCES

ACAR, Y.B., BURGUNOGLU, H.T. and TUMAY, M.T. (1982). Interface Propeties of Sand, *Journal of the Geotechnical Engineering Division*, ASCE, Vol. 108, GT4, pp. 648-654.

BAKEER, R.M. and BHATIA, S.K. (1989). Earth Pressure Behind a Gravity Retaining Wall, *International Journal for Numerical and Analytical Methods in Geomechanics*, Vol. 13, pp. 665-673.

BOLTON, M.D., SPRINGMAN, S.M. and SUN, H.W. (1990). The Behavior of Bridge Abutments on Clay, *Proceedings of the ASCE Specialty Conference on Design and Performance of Earth Retaining Structures*, Cornell University, New York, pp. 292-306.

CIVIL ENGINEERING CODE OF PRACTICE NO. 2 (1951). *Earth Retaining Structures*, BSI, London.

CLAYTON, C.R.I. and MILITITSKY, J. (1986). *Earth Pressure and Earth-Retaining Structure*, Surrey University Press, Glasgow.

CLOUGH, G.W. (1969). Finite Element Analyses of Soil-Structure Interaction in U-Frame Locks, thesis presented to the University of California, Berkeley, in partial fulfilment of the requirements for the degree of Doctor of Philosophy.

CLOUGH, G.W. and DUNCAN, J.M. (1971). Finite Element Analyses of Retaining Wall Behavior, *Journal of the Soil Mechanics and Foundation Engineering Division*, ASCE, Vol. 9, SM12, pp. 1657-1673.

COULOMB, C.A. (1776). Essai sur une Application des regles des Maximums et Minimums a Quelques Problemes de Statique Relatifs a L'architecture, *Memoirs Academie Royal des Sciences*, Vol. 3, pp. 38.

DUNCAN, J.M., CLOUGH, G.W. AND EBERLING, R. (1990). Behavior and Design of Gravity Earth Retaining Structures, *Proceedings of the ASCE Specialty Conference on Design and Performance of Earth Retaining Structures*, Cornell University, New York, pp. 251-277.

GOH, A.T.C. (1993). Behavior of Cantilever Retaining Walls, *Journal of the Geotechnical Engineering Division*, ASCE (in print).

GOODMAN, R.E., TAYLOR, R.L. and BREKKE, T.L. (1968). A Model for the Mechanics of Jointed Rock, *Journal of the Soil Mechanics and Foundation Engineering Division*, ASCE, Vol. 94, SM3, pp. 637-659.

KULHAWY, F.H. (1974). Analysis of a High Gravity Retaining Wall, *Proceedings of the ASCE Conference on Analysis and Design in Geotechnical Engineering*, University of Texas, Austin, Vol. 1, pp. 159-172.

NAKAI, T. (1985). Finite Element Computations for Active and Passive Earth Pressure Problems on Retaining Wall, *Soils and Foundations*, Vol. 25, No. 3, pp. 98-112.

NAYAK, G.C. and ZIENKIEWICZ, O.C. (1972). Elasto-Plastic Stress Analysis. A Generalisation of Various Constitutive Relations Including Strain-Softening, *International Journal of Numerical Methods in Engineering*, Vol. 5, No. 1, pp. 113-135.

RANKINE, W.J.M. (1857). On the Stability of Loose Earth, *Philosophical Transactions of the Royal Society*, Vol. 147, pp. 9-27.

SEED, R.B. and DUNCAN, J.M. (1986). FE Analyses : Compaction-Induced Stresses

and Deformations, *Journal of the Geotechnical Engineering Division,* ASCE, Vol. 112, GT1, pp. 23-43.

TERZAGHI, K. (1954). Anchored Bulkheads. *Transactions* ASCE, Vol. 119, pp. 1243-1280.

TERZAGHI, K. and PECK, R.B. (1948). *Soil Mechanics in Engineering Practice.* 1st edition. John Wiley, New York.